

Status of Lattice Studies of the QCD Phase Diagram

Owe PHILIPSEN^{*)}

*Institut für Theoretische Physik, Westfälische Wilhelms-Universität Münster,
48149 Münster, Germany*

Determining the QCD phase diagram is a pressing task in view of its relevance for nuclear and astro-particle physics programmes. We review the current status of lattice calculations of the phase diagram in the (T, μ_B) -plane for baryon chemical potentials $\mu_B \lesssim 500$ MeV. At $\mu_B = 0$, simulations of staggered fermion actions predict the quark hadron transition to be a crossover in the continuum limit. As a baryon chemical potential is turned on, there is mounting evidence on coarse lattices for the crossover to weaken, rather than turning into a true phase transition at a critical point, as predicted by earlier simulations.

§1. Introduction

The QCD phase diagram has been the subject of intense research over the last ten years. Once fully determined, it will locate the regions of different forms of nuclear matter in the parameter space spanned by temperature T and baryon chemical potential μ_B . Based on the fundamental property of asymptotic freedom, one expects at least three different regions: hadronic (low μ_B, T), quark gluon plasma (high T) and colour-superconducting (high μ_B , low T). For chemical potentials exceeding $\mu_B \gtrsim 1$ GeV, the situation may be more complicated with possible additional phases.¹⁾

Unfortunately, a quantitative calculation of the phase diagram from first principles is extraordinarily difficult. Since QCD is strongly coupled on scales $\lesssim 1$ GeV, lattice simulations are the only tool to eventually give reliable answers, provided that systematic errors are controlled. As we shall see, at present it is still a long way to achieve this goal. In fact, lattice investigations at finite density are hampered by the “sign problem”, and only approximate methods are available that work at small quark densities, $\mu = \mu_B/3 \lesssim T$.^{2),3)} This adds further systematic errors to those known from zero density thermodynamics, like finite volume and discretisation effects. Accordingly, in this contribution we shall only consider the quark hadron transition at small densities. The widely accepted expectation is for a finite density first order phase transition terminating in a critical endpoint, and an analytic crossover behaviour at $\mu = 0$ (cf. Fig. 3 (right)).

In the absence of first principles calculations, where did this picture come from? It is based on combining lattice results for $\mu = 0$ in the larger parameter space $\{m_{u,d}, m_s, T\}$ with model calculations at $\mu \neq 0$ ⁴⁾ and connecting various limiting cases by universality and continuity arguments.⁵⁾ The schematic situation is depicted in Fig. 1. In the limits of zero and infinite quark masses (lower left and upper right corners), order parameters corresponding to the breaking of a global symmetry can

^{*)} in collaboration with Ph. de Forcrand (ETH Zürich/CERN)

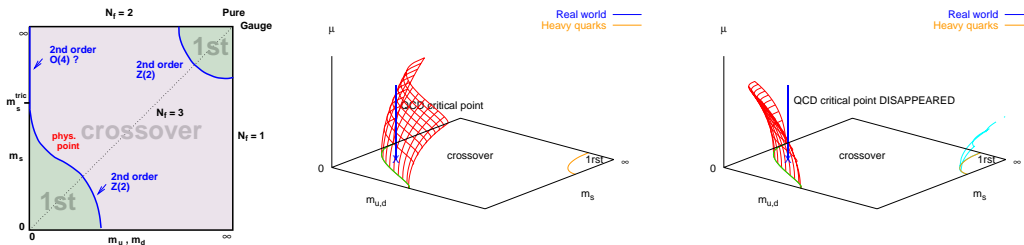


Fig. 1. Left: Schematic phase transition behaviour of $N_f = 2+1$ QCD for different choices of quark masses ($m_{u,d}, m_s$) at $\mu = 0$. Middle/Right: Critical surface swept by the chiral critical line as μ is turned on. Depending on the curvature, a QCD chiral critical point is present or absent. For heavy quarks the curvature has been determined⁸⁾ and the first order region shrinks with μ .

be defined, and one numerically finds first order phase transitions at small and large quark masses at some finite temperatures $T_c(m)$. On the other hand, one observes an analytic crossover at intermediate quark masses, with second order boundary lines separating these regions. Both lines have been shown to belong to the $Z(2)$ universality class of the 3d Ising model.^{6)–8)}

The “derivations” of the generally expected QCD phase diagram⁵⁾ state two crucial assumptions: a) the chiral transition for $N_f = 2$ is second order and thus in the $O(4)$ universality class, which implies the existence of a tricritical point at some strange quark mass m_s^{tric} ; b) by switching on μ , this point will continuously move to larger m_s until it ends up as a tricritical point for the $N_f = 2$ theory at some finite μ_{tric} . Similarly, for small but non-zero $m_{u,d}$, the $Z(2)$ chiral critical line would continuously shift with μ until it passes through the physical point at μ_E , corresponding to the endpoint of the QCD phase diagram. This is depicted in Fig. 1 (middle), where the critical point is part of the chiral critical surface. Note, however, that there is no a priori reason for this. In principle it is also possible for the chiral critical surface to bend towards smaller quark masses, cf. Fig. 1 (right), in which case there would be no chiral critical point or phase transition at moderate densities. In the sequel the lattice evidence for these scenarios will be reviewed.

§2. $N_f = 2$ at zero density

Let us first consider assumption a) above. Since the cost of dynamical simulations explodes with shrinking quark masses, the order of the two-flavour chiral transition is even harder to determine than that of physical QCD. Despite many attempts it could not yet be conclusively settled. Wilson fermions appear to see $O(4)$ scaling,⁹⁾ while staggered actions are inconsistent with $O(4)$ and $O(2)$ (for the discretised theory).¹⁰⁾ A recent finite size scaling analysis using staggered fermions with unprecedented lattice sizes was performed in.¹¹⁾ Again, these data appear inconsistent with $O(4)/O(2)$, and the authors conclude a first order transition to be more likely. A different conclusion was reached in,¹²⁾ in which χ QCD was investigated numerically. This is a staggered action modified by an irrelevant term (i.e. one going to zero in the continuum limit) such as to allow simulations in the chiral limit. The

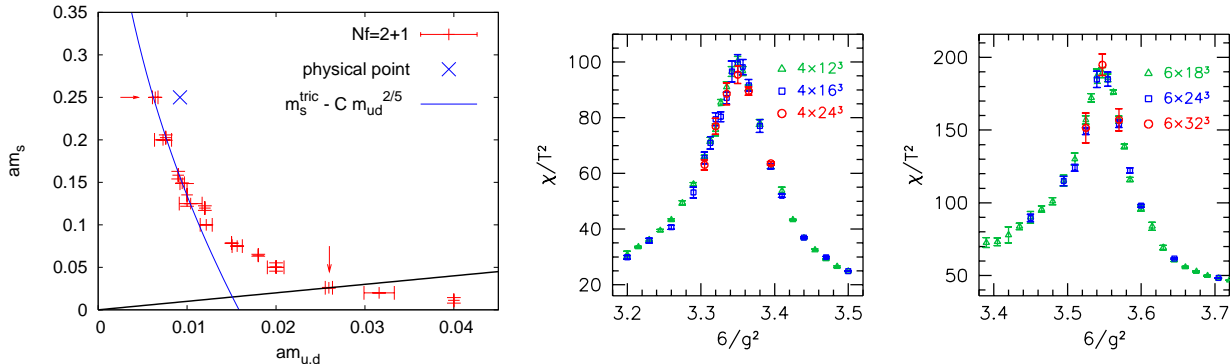


Fig. 2. Left: The chiral critical line in the bare mass plane at $\mu = 0$. $N_f = 3$ corresponds to the solid line. Also shown is a fit to an assumed tricritical point, $m_s^{tric} \sim 2.8T$.¹⁵⁾ Right: Finite size scaling of the chiral susceptibility at the physical point for $N_t = 4, 6$. The peaks saturate at a finite value, consistent with crossover behaviour.¹⁶⁾

authors find their data compatible with those of an $O(2)$ spin model on moderate to small volumes. They thus suspect that finite volume effects of current $N_f = 2$ QCD simulations mask the correct scaling.

Finally, from universality of chiral models it is known that the order of the chiral transition is related to the strength of the $U_A(1)$ anomaly.¹³⁾ In a model constructed to have the right symmetry with a tunable anomaly strength, it has recently been demonstrated non-perturbatively that both scenarios are possible, with a strong anomaly required for the chiral phase transition to be second order.¹⁴⁾

Thus, we cannot yet take assumption a) for granted. Should the chiral transition turn out to be first order, the likely modification of Fig. 1 (left) would be the disappearance of the tricritical point, with the chiral critical line intersecting the $N_f = 2$ axis at some finite $m_{u,d}$ and being $Z(2)$ all the way. Provided this line shifts to the right with μ as in assumption b), the (T, μ_B) -phase diagram for physical QCD would still look as expected. But contrary to the scenario in Ref.,⁵⁾ its critical point would be unrelated to any tricritical point.

§3. The chiral critical line at $\mu = 0$

The boundary line between the chiral first order and crossover regions has recently been mapped out on $N_t = 4$ lattices,¹⁵⁾ Fig. 2 (left). A convenient observable is the Binder cumulant $B_4(X) \equiv \langle (X - \langle X \rangle)^4 \rangle / \langle (X - \langle X \rangle)^2 \rangle^2$, with $X = \bar{\psi}\psi$. At the second order transition, B_4 takes the value 1.604 dictated by the $3d$ Ising universality class. In agreement with expectations, the critical line steepens in approaching the chiral limit. Assuming a tricritical point on the m_s -axis according to Fig. 1 (left), the critical line is in fact consistent with tricritical scaling with $m_{u,d}$ ⁵⁾ and allows to estimate $m_s^{tric} \sim 2.8T_c$. Note however, that this estimate is extremely cut-off sensitive and would change considerably on a finer lattice.

The most important question concerns the location of the physical point, which is marked by the cross in Fig. 2 (left). As expected, it is on the crossover side of the

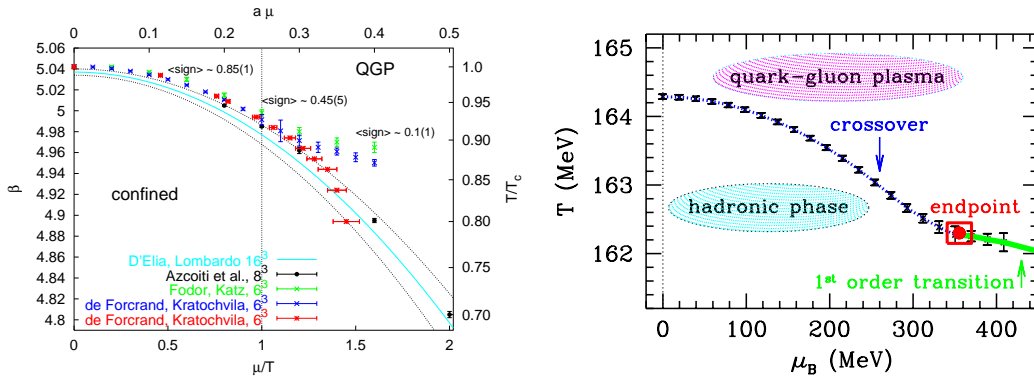


Fig. 3. Left: Comparison of different methods to compute the critical couplings.²⁰⁾ Right: Phase diagram for physical quark masses as predicted by two parameter reweighting on $N_t = 4$.²³⁾

critical line. In Ref. 15) ratios of pion to rho and kaon masses were evaluated on the points marked by arrows, to ensure that this statement indeed carries over from bare quark masses to the spectrum of physical particles. Quark masses being extremely susceptible to renormalisation effects, it is important to check this situation on finer lattices. This has been completed in Ref. 16) by a slightly different strategy. Here, the authors tune the quark masses to the physical theory and then perform a finite size scaling analysis of susceptibilities around the critical temperature, viz. lattice coupling. This is shown in Fig. 2 (right) for different lattice spacings. Clearly, the peaks saturate at a finite value which can be extrapolated to the continuum. This quite convincingly shows physical QCD to exhibit an analytic crossover rather than a true phase transition at zero density. The only remaining caveat to this conclusion would be if there was a fundamental problem with the so-called rooting trick when using staggered fermions, as frequently debated.¹⁷⁾ Similar calculations using Wilson fermions could close this gap soon.

In an attempt to control cut-off effects, also the critical line has been checked on finer $N_t = 6$ ($a \sim 0.2$ fm) lattices. The results show an important shift of the critical line towards the origin: for the $N_f = 3$ theory, the pion mass, measured at $T = 0$ with the critical quark mass, decreases from $1.6 T_c$ to $0.95 T_c$.¹⁸⁾ Similar results are reported for $N_f = 2 + 1$.¹⁹⁾ Since cut-off effects on the physical point are much milder, this considerably increases the distance of the critical surface to the physical point, Fig. 1. Regardless of the sign of the curvature, this trend alone makes a QCD chiral critical point at small $\mu/T \lesssim 1$ less likely.

§4. Calculations at finite density

Straightforward Monte Carlo simulations at finite baryon density are impossible. This is because the fermion determinant becomes complex for non-vanishing μ , prohibiting its use as a probability weight in Monte Carlo algorithms. This fact is also known as the “sign-problem”.

There is a number of methods that circumvent the sign problem, rather than

N_f	am	N_s	t_2	Action	β -Function	Method	Reference
2	0.1	16	0.69(35)	p4	non-pert.	Taylor+Rew.	²²⁾
	0.025	6,8	0.500(34)	stag.	2-loop pert.	Imag.	²⁴⁾
3	0.1	16	0.247(59)	p4	non-pert.	Taylor+Rew.	²²⁾
	0.026	8,12,16	0.667(6)	stag.	2-loop pert.	Imag.	¹⁵⁾
	0.005	16	1.13(45)	p4	non-pert.	Taylor+Rew.	²²⁾
4	0.05	16	0.93(9)	stag.	2-loop pert.	Imag.	²¹⁾
2+1	0.0092,0.25	6-12	0.284(9)	stag.	non-pert.	Rew.	²³⁾

 Table I. Coefficient t_2 in the Taylor expansion of the transition line, Eq. (4.1) from $N_t = 4$.

solving it: i) Multi-parameter reweighting, ii) Taylor expansion in $(\mu/T)^2$ around $\mu = 0$ (even powers because of CP invariance) and iii) simulations at imaginary chemical potential, either followed by analytic continuation or Fourier transformed to the canonical ensemble. All of these introduce some degree of approximation. However, the systematic errors are rather different, thus allowing for powerful crosschecks. Reviews specialized on the technical aspects can be found in Refs. 2), 3).

The first task is to identify the phase boundary, i.e. the critical coupling and thus $T_c(\mu)$. This has been done for a variety of flavours and quark masses using different methods. For a quantitative comparison one needs data at one fixed parameter set. Such a comparison is shown for the critical coupling in Fig. 3 (left), for $N_f = 4$ staggered quarks with the same action and quark mass $m/T = 0.2$. (For that quark mass the transition is first order along the entire curve). One observes quantitative agreement up to $\mu/T \approx 1.3$, after which the different results start to scatter. Thus, all methods appear to be reliable for $\mu/T \lesssim 1$, or $\mu_B \lesssim 500$ MeV. The case of physical quark masses, after conversion to continuum units, is shown in Fig. 3 (right).²³⁾ One observes that T_c is decreasing only very slowly with μ . This is consistent with a description by a series in $(\mu/\pi T)^2$ with coefficients of order one,

$$\frac{T_c(\mu)}{T_c(0)} = 1 - t_2(N_f, m_f) \left(\frac{\mu}{\pi T}\right)^2 + \mathcal{O}\left(\left(\frac{\mu}{\pi T}\right)^4\right) . \quad (4.1)$$

The leading coefficients for various cases have been collected from the literature³⁾ and are reproduced in Table I. The curvature grows with N_f , which is consistent with $\sim N_f/N_c$ behaviour found in large N_c expansions.²⁵⁾ Subleading coefficients are emerging at present but not statistically significant yet. Note that continuum conversions relying on the two-loop beta function are certainly not reliable for these coarse lattices, while fits to non-perturbative beta functions tend to increase the curvature.

§5. The chiral critical surface

All methods mentioned here also give signals for criticality, but the comparison is non-trivial because of different parameter sets. A simulation using reweighting methods on $N_t = 4$ lattices puts the critical point at $\mu_B^E \sim 360$ MeV,²³⁾ Fig. 3 (right), supporting the standard expected scenario. Quark masses were tuned to

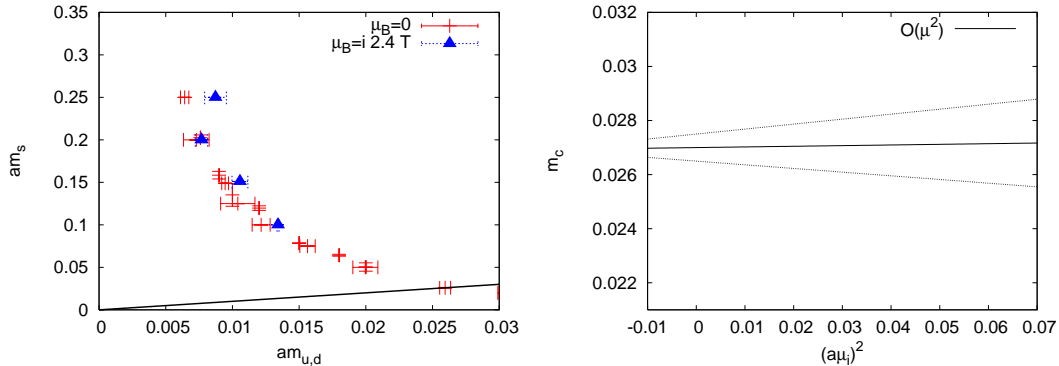


Fig. 4. Left: Chiral critical line at zero and non-zero imaginary μ . Right: One sigma error band for the $N_f = 3$ critical mass $am^c(\mu)$ resulting from a leading order fit. Both for $N_t = 4$.¹⁵⁾

give the ratios $m_\pi/m_\rho \approx 0.19$, $m_\pi/m_K \approx 0.27$, which are close to their physical values. In principle the determination of a critical point is also possible via the Taylor expansion, where a true phase transition will be signalled by a finite radius of convergence for the pressure series about $\mu = 0$ as the volume is increased. A critical endpoint for the $N_f = 2$ theory, based on this approach, was reported in²⁶⁾ for bare quark mass $m/T_c = 0.1$. Taking the measured first four coefficients for the asymptotic behaviour of the series, the estimate for the location of the critical point is $\mu_B^E/T_E = 1.1 \pm 0.2$ at $T_E/T_c(\mu = 0) = 0.95$.

Rather than fixing a theory with a particular set of quark masses and then switching on a chemical potential, let us now try to learn about the phase structure in the extended parameter space $\{m_{u,d}, m_s, T, \mu\}$, i.e. map out the chiral critical surface. This has been done for $N_t = 4$ lattices using simulations at imaginary chemical potential.¹⁵⁾ Fig. 4 shows a comparison of the chiral critical line at zero density and a few points at imaginary chemical potential $\mu_B = i2.4T$. The finite density effect is very small, consistent with what is found for the change of the critical temperature, Eq. (4.1). Thus, the critical surface in Fig. 1 appears to emerge very steeply from the quark mass plane, making the critical point of physical QCD extremely quark mass sensitive.

The critical surface for imaginary μ , Fig. 4, is moving to larger quark masses. What does this imply for real chemical potential? To answer this question we focus on $N_f = 3$, collecting data for several values of μ_i . Since $\mu_i/T \lesssim 1$, the critical quark mass may be Taylor expanded $am^c(\mu) = am_0^c + c_1'(a\mu)^2 + \dots$, and the coefficients can be fitted to the data at imaginary μ . Fig. 4 (right) shows a one sigma error band for the critical bare quark mass from a leading order fit. As observed before, the μ -dependence is very weak and even consistent with zero for these errors. Since $T(\mu) = 1/(a(\mu)N_t)$, $a(\mu)$ is an increasing function on a given lattice, so that the critical mass in fixed physical units shrinks with μ , as in Fig. 1 (right).

One may worry about systematic errors when fitting a leading order polynomial to data containing the full functional dependence. For example, subsequent terms may be cancelling in the imaginary, but not in the real direction.

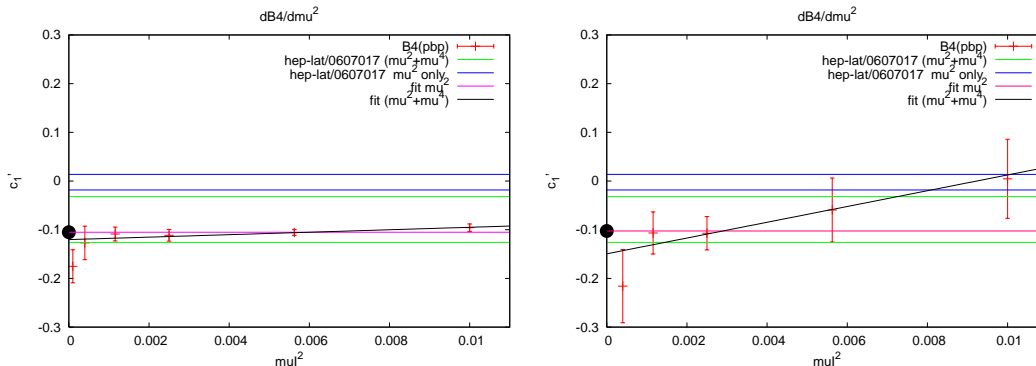


Fig. 5. Leading μ^2 -derivatives of the critical quark mass on $N_t = 4$ on $L = 8$ (left) and $L = 12$ (right). The error bands give the corresponding values of LO and NLO fits to Taylor series.¹⁵⁾

In order to check this, we have also calculated the leading derivative directly via $c'_1 = -\partial_{(a\mu)^2} B_4 / \partial_{am} B_4$. We do this in a novel, efficient way by evaluating finite differences

$$\frac{\partial B_4}{\partial (a\mu)^2} = \lim_{(a\mu)^2 \rightarrow 0} \frac{B_4(a\mu) - B_4(0)}{(a\mu)^2}. \quad (5.1)$$

Because the required shift in the couplings is very small, it is adequate and safe to use the original Monte Carlo ensemble for $am_0^c, \mu = 0$ and reweight the results by the standard Ferrenberg-Swendsen method. Moreover, by reweighting to imaginary μ the reweighting factors remain real positive and close to 1. The results of this procedure based on 5 million trajectories on $8^3, 12^3 \times 4$, are shown in Fig. 5 for two volumes. Subleading terms show up as a slope in the linear extrapolation. Indeed, such a slope is visible in Fig. 5 (right). Both coefficients are consistent with the results from the finite μ_i calculations, provided the next-to-leading order is taken into account. We have also continued to collect statistics for the imaginary μ simulations, so we now have two significant terms. Putting everything together, our current best estimate for $N_f = 3$ on $N_t = 4$ lattices is

$$\frac{m_c(\mu)}{m_c(0)} = 1 - 3.3(5) \left(\frac{\mu}{\pi T}\right)^2 - 12(6) \left(\frac{\mu}{\pi T}\right)^4 + \dots \quad (5.2)$$

The emerging μ^4 -term is negative as well, further shrinking the first order region with increasing μ . On $N_t = 4$ lattices, there is thus little doubt that the scenario Fig. 1 (right) is realised for $\mu_B \lesssim 500$ MeV. Note that this is analogous to the situation with heavy quarks, where the first order transition is also weakening with μ .⁸⁾

§6. Discussion

Our result for the chiral critical surface appears to be in contradiction with the phase diagram obtained from reweighting methods, Fig. 3. As explained above, we have checked with independent methods that the signs we find for our coefficients are not artefacts of the fitting procedure. On the other hand, there are concerns

that the critical point determined via reweighting falls into a parameter range where reweighting becomes problematic.²⁷⁾ However, even disregarding those, the bare lattice results of Refs. 15), 23) are not necessarily inconsistent. Reweighting in μ is performed for fixed quark masses in lattice units, am_q . Since $T(\mu) = 1/(aN_t)$, $a(\mu)$ is an increasing function on a given lattice, hence the critical point observed by reweighting corresponds to quark masses smaller than physical. Indeed, Fig. 2 shows that on $N_t = 4$ the physical point is very close to the critical surface. This is a discretisation effect, and simulations on finer lattices are required in order to settle the issue. As discussed above, we know already that the distance between the critical surface and the physical point grows significantly, making a chiral critical point at small μ_B less likely, irrespective of the curvature of $m_c(\mu)$. Calculations of the curvature on $N_t = 6$ are currently in progress.

References

- 1) K. Rajagopal and F. Wilczek, arXiv:hep-ph/0011333.
- 2) O. Philipsen, PoS **LAT2005** (2006) 016 [PoS **JHW2005** (2006) 012] [arXiv:hep-lat/0510077].
- 3) C. Schmidt, PoS **LAT2006** (2006) 021 [arXiv:hep-lat/0610116].
- 4) M. A. Stephanov, Prog. Theor. Phys. Suppl. **153** (2004) 139 [Int. J. Mod. Phys. A **20** (2005) 4387] [arXiv:hep-ph/0402115].
- 5) A. M. Halasz *et al.*, Phys. Rev. D **58** (1998) 096007 [arXiv:hep-ph/9804290]. M. A. Stephanov, K. Rajagopal and E. V. Shuryak, Phys. Rev. Lett. **81** (1998) 4816 [arXiv:hep-ph/9806219].
- 6) F. Karsch, E. Laermann and C. Schmidt, Phys. Lett. B **520** (2001) 41 [arXiv:hep-lat/0107020].
- 7) P. de Forcrand and O. Philipsen, Nucl. Phys. B **673** (2003) 170 [arXiv:hep-lat/0307020].
- 8) S. Kim, Ph. de Forcrand, S. Kratochvila and T. Takaishi, PoS **LAT2005**, (2006) 166 [arXiv:hep-lat/0510069].
- 9) A. Ali Khan *et al.* [CP-PACS Collaboration], Phys. Rev. D **63** (2001) 034502 [hep-lat/0008011]; Y. Iwasaki *et al.*, Phys. Rev. Lett. **78** (1997) 179 [hep-lat/9609022].
- 10) C. W. Bernard *et al.* [MILC Collaboration], Phys. Rev. D **61** (2000) 111502 [hep-lat/9912018]; E. Laermann, Nucl. Phys. Proc. Suppl. **60A** (1998) 180.
- 11) M. D’Elia, A. Di Giacomo and C. Pica, Phys. Rev. D **72** (2005) 114510 [hep-lat/0503030]; G. Cossu, M. D’Elia, A. Di Giacomo and C. Pica, [arXiv:0706.4470 [hep-lat]].
- 12) J. B. Kogut and D. K. Sinclair, Phys. Rev. D **73** (2006) 074512 [hep-lat/0603021].
- 13) R. D. Pisarski and F. Wilczek, Phys. Rev. D **29**, 338 (1984).
- 14) S. Chandrasekharan and A. C. Mehta, [arXiv:0705.0617 [hep-lat]].
- 15) P. de Forcrand and O. Philipsen, JHEP **0701** (2007) 077 [hep-lat/0607017].
- 16) Y. Aoki *et al.*, Nature **443** (2006) 675 [hep-lat/0611014].
- 17) M. Creutz, PoS **LATTICE2007** (2006) 007 [arXiv:0708.1295 [hep-lat]]. A. S. Kronfeld, PoS **LATTICE2007** (2006) 016 [arXiv:0711.0699 [hep-lat]].
- 18) P. de Forcrand, S. Kim and O. Philipsen, PoS **LAT2007** (2007) 178 [arXiv:0711.0262 [hep-lat]].
- 19) G. Endrodi *et al.*, PoS **LAT2007** (2007) 182 [arXiv:0710.0998 [hep-lat]].
- 20) P. de Forcrand and S. Kratochvila, PoS **LAT2005** (2006) 167 [hep-lat/0509143].
- 21) M. D’Elia and M. P. Lombardo, Phys. Rev. D **67** (2003) 014505 [hep-lat/0209146].
- 22) C. R. Allton *et al.*, Phys. Rev. D **66** (2002) 074507 [arXiv:hep-lat/0204010]. Nucl. Phys. Proc. Suppl. **129** (2004) 614 [hep-lat/0309116].
- 23) Z. Fodor and S. D. Katz, JHEP **0404** (2004) 050 [arXiv:hep-lat/0402006].
- 24) P. de Forcrand and O. Philipsen, Nucl. Phys. B **642** (2002) 290 [arXiv:hep-lat/0205016].
- 25) D. Toublan, arXiv:hep-th/0510090.
- 26) R. V. Gavai and S. Gupta, Phys. Rev. D **71** (2005) 114014 [arXiv:hep-lat/0412035].
- 27) K. Splittorff, arXiv:hep-lat/0505001. J. Han and M. A. Stephanov, arXiv:0805.1939 [hep-lat].